0638

Incorporating Geostatistical Methods with Monte Carlo Procedures for Modeling Coalbed Methane Reservoirs

Reinaldo J. Gonzalez, Advanced Resources International Inc.
Aiysha Sultana, Advanced Resources International Inc.
Anne Y. Oudinot, Advanced Resources International Inc.
Scott R. Reeves, Advanced Resources International Inc.

ABSTRACT

Coalbed methane (CBM) and other non-conventional gas plays have become an important factor in the United States energy market, and present real engineering challenges for characterization and exploitation. Due to the heterogeneity of these reservoirs, their productivity depends upon an inter-related set of reservoir, completion and production characteristics. Reservoir modeling production predictions involve considerable uncertainty, and one must take into account multiple scenarios to find the best exploitation plans. Tools are therefore needed to identify the most important geologic and engineering factors, and to quantify the range of variability in uncertain variables.

Due to the high uncertainty present in the analyzed cases, reservoir simulation coupled with stochastic methods, i.e., Monte Carlo procedures, has provided an excellent methodology to predict production profiles with a wide variety of reservoir character and producing conditions. Expanding the scope of this initial approach, geostatistical methodologies have been utilized in order to incorporate alternative spatial distributions of the most relevant reservoir parameters. In this paper, geostatistical approaches are presented, with the encouraging results related to a real field case.

INTRODUCTION

Risk and uncertainty are key aspects of most oil industry problems and need to be understood for any decision-making process. Reservoir modeling groups have to make predictions facing constant uncertainty, or take into account multiple scenarios to find the most appropriate exploitation plans. These requirements mean that tools are needed to identify the most important geologic and engineering factors and to quantify the range of uncertainty in outcomes such as cumulative production, maximum rates or net present value.

Quantitative risk analysis applying Monte Carlo (MC) simulation methods provide a powerful tool for quantifying the various types of uncertainty. The uncertainty is addressed by generating a large number of simulations, changing values inside the range of uncertainty in geologic, engineering and other important parameters. MC procedures provide the reservoir analyst the option of describing risk and uncertainty in the form of probabilistic distributions of values corresponding to those model parameters considered uncertain and/or unknown.

From an unconventional reservoir viewpoint, simulation projects typically require multiple executions to reach conclusions (sometimes unsatisfactory) about the productivity of a reservoir. Depending on the

complexity of the problem, the time to reach these possible answers could range from hours to weeks or months of simulation time. This is a situation that can be tackled more efficiently by using MC techniques coupled with a Dynamic Simulator (DS).

This topic has been an object of study for already some time, in particular for conventional reservoirs [1,2,3]. However, few experiences applied to CBM and other types of unconventional reservoirs can be found in literature[4,5]. Oudinot et al reported a MC-DS procedure called SPEcieS which is successfully applied to forecast production on CBM reservoirs and other unconventional plays.

Geostatistics is generally applied to obtaining more realistic reservoir characterizations, which honors geological spatial behavior and considers rock heterogeneities. The inclusion of geostatistical characterizations of reservoir parameters into the coupled MC-DS procedure can, likewise, be found in literature for conventional reservoirs where methods based on experimental design are frequently applied[6,7,8]. However, to the knowledge of these authors, this geostatistical inclusion is rarely applied to reservoir simulation of unconventional plays, and is the objective of this study.

Due to the high uncertainty present in CBM cases, a fractured reservoir simulator, COMET3 [5], has been coupled to stochastic methods to provide an excellent resource to generate production profiles using a wide variety of possibilities about reservoir character and producing conditions. The coupled MC-DS procedure developed here includes the consideration of main geostatistical parameters for describing the spatial behavior of permeability. This procedure is used to generate several hundred possible combinations of the uncertain reservoir variables, which became inputs to COMET3 simulations.

The resulting forecasts are used in two types of sensitivity study. Firstly, from a phenomenological point of view, seeking to determine which factors (for example, permeability, fracture spacing, spatial anisotropy coefficient, or sorption time) determine production behavior and recovery volumes. On the other hand, an uncertainty study predicts the range of possible outcomes, usually in terms of significant production variables such as cumulative total gas or water rate.

In this paper, we focused on understanding the variability in the production response when geostatistical characterizations of main reservoir parameters are used to populate a DS grid. Permeability (average) and porosity (fracture) constituted the main variables to be studied in this initial research; however, other possibilities like saturations, thickness, etc., can be considered. Particular attention was paid on permeability and its effect on gas production which is especially valuable for exploitation design and financial analysis.

ABOUT GEOSTATISTICS

In order to populate the COMET3 simulation grid with permeability values geostatistically generated, it was necessary to make some practical implementation decisions.

The geostatistical permeability characterizations used in this experiment were generated applying programs from the GSLIB[9] package. GSLIB (Geostatistical Software Library) is a public domain collection of programs developed and used at Stanford University over the course of 26 years of their Post Graduate Programs, and it has received a large acceptance both in industry, for their practical applications, and in academia, due to its flexibility to experiment with new ideas.

Another important issue was which geostatistical parameters should be considered the most important for this kind of application? Four parameters were taken into account being related with the key geostatistical tool for capturing and modeling the spatial behavior of a reservoir parameter, i.e., the semivariogram[9,10]. These parameters were nugget effect, azimuth (the direction of maximum spatial autocorrelation), range (maximum distance of spatial autocorrelation reached at azimuth), and anisotropy coefficient (ratio between range and the distance of minimum spatial correlation presumably reached at a direction perpendicular to azimuth). All these parameters are directly linked with the main geostatistical manner of

modeling spatial anisotropy of a reservoir parameter which is based on a geometric analogy with ellipses (or ellipsoids). Nugget effect is usually interpreted as geologic noise and is conceived as combination of sampling errors and sources of variation operating over smaller scales where instruments were not capable to measure[9,10].

Another question was what kind of stochastic simulation algorithm should be used. The most straightforward algorithm for generating geostatistical characterizations of a reservoir parameter is given by the Sequential Gaussian Simulation (SGS) approach. In spite of its advantages that have made it very popular, this algorithm could be inadequate in terms of other important issues related to geological facts, so future research is programmed with the utilization of other stochastic simulation technique.

A theoretical semivariogram model needed to be adopted. This particular issue was handled using the spherical model[9,10] which depends basically on the four parameters above mentioned. This theoretical model is commonly used in reservoir modeling practice, and constitutes for geostatistics what the normal distribution represents for statistics.

A final important issue was to preserve the advantages of geostatistical characterizations in more coarse COMET3 grids with the less impact over the modeled spatial behavior and the heterogeneous character of the reservoir parameter description. In other words, to face the still open problem of upscaling permeability values from a geostatistical fine mesh to a coarse DS mesh. For these experiments, it was decided to adapt the geostatistical grid definition to a balanced definition of the COMET3 grid. Then, in order to utilize a regular grid on geostatistical simulations, statistically representative sizes were adopted based on the COMET3 mesh definition.

DISCUSSION

A real unconventional gas play (shale) was considered for this paper. In all analyzed cases, a square region of 160 acres was utilized with the presence of a vertical well in the middle of this region. Some reservoir, completion and production information coming from this unconventional gas play was used but has been omitted here for confidentiality reasons.

For the DS part, the reservoir was initially described as a one-layer reservoir of 44 feet thickness (two-dimensional case). An irregular simulation grid was proposed of dimensions 23 x 23 x 1, where the length of each grid block is based on the length of the grid block in which the well is located (middle block) and an increment factor necessary to compute the length of each consecutive grid block. In other words small grid blocks at the well and its neighborhood, and grid blocks gradually incrementing in dimensions as they were approaching to the reservoir boundaries.

The uncertain variables for this study were

- Initial Water Saturation (SW_0)
- Average Permeability (AP)
- Permeability Anisotropy Factor (between K_X and K_Y)
- Fracture Porosity (FP)
- Sorption Time
- Fracture Spacing
- Langmuir Volume
- Langmuir Pressure
- Water Density
- Skin Factor
- Desorption Pressure Function (Pd/Pi)
- Irreducible Water Saturation (Swr)
- Maximum gas relative permeability (KrgMax)
- Corey gas exponent (KrgExp)

- Corey water exponent (KrwExp)

Last four parameters on this list are related with Corey formulas for relative permeability. Average Permeability (AP) is used to generate values of K_X and K_Y (x-direction permeability and y-direction permeability respectively). There is no limitation to the number of parameters that can be varied; indeed, most other simulator input parameters can also be probabilistically varied.

Uncertain parameters were then assigned distribution types. These functions simply represent a range of different possible values that a parameter could take instead of limiting it to just one value. Types of statistical distributions mostly used are lognormal, normal, triangular and uniform.

In this study, most of statistical decisions about models and their intrinsic parameters were based on available reservoir information and analyst team experience. Table 1 shows, for each variable, the adopted statistical model with their respective statistical parameters. We define the following notation:

- N(a, b): Normal distribution with mean value = a, and standard deviation = b
- L(a, b): Lognormal distribution with mean value = a, and standard deviation = b
- T(a, b, c): Triangular distribution with minimum value = a, most likely value = b, and maximum value = c

The cumulative gas production was selected like the key output parameter for subsequent analyses. Water production, gas rate and water rate were other output parameters. Equivalent analyses and results can be derived from water production. Analyses were supported mainly on summary statistics, histograms and sensitivity charts (Tornado plots) which were used in order to elucidate those parameters that impact the production response on the investigated case.

After all the assumptions were made on the desired parameters and all outputs were defined, a conventional process MC-DS was firstly executed (for more details, see Oudinot[5]) and results are presented in Case Study 1. At the end of all simulations, descriptive statistics and Tornado plots were generated to analyze and rank the impact that uncertain parameters have on gas production.

Case Study 1

(Homogeneous permeability distribution)

The objective of this first exercise was to have the reference case where a conventional MC-DS procedure is applied, i.e., without any geostatistical consideration. In other words, all input parameters above mentioned were randomly varied according their respective statistical models and, in particular, permeability was homogeneously distributed for each realization.

Generating a Tornado plot on the cumulative gas production identified AP and Fracture Porosity (FP) as the main performance drivers as shown on Figure 1. Note that variables impacting cumulative gas production the most are at the top of the chart. Tornado plots are based on rank correlation coefficients.

Figure 2 shows the relative frequency histogram of cumulative total gas with some related statistic values. Mean and median values of Cumulative Total Gas responses are 385,804 Mscf and 355,526 Mscf respectively; so it can be said that central values are around 370,000 Mscf. The maximum simulated value for this case was 1,142,973.80 Mscf. From the corresponding Cumulative Probability Distribution (CPD) curve shown in Figure 3, we can obtain, for instance, that probability of gas production being greater than 500,000 Mscf is 0.24.

In essence, all these values have been taken as initial references for subsequent experiments and analyses.

Case Study 2
(Homogeneous and heterogeneous permeability distribution)

In order to facilitate analyses about the incorporation of reservoir parameters characterized geostatistically into a MC-DS procedure, the next experiment was focused only in randomly varying AP values (consequently K_X and K_Y) and how they are spatially utilized in the simulation grid.

Firstly, base values were adopted for all uncertain parameters above listed except AP. These base values were either the most likely or the mean value depending on which statistical model had been adopted for each input parameter in Case 1 (Table 1).

Again, a conventional MC-DS procedure was executed randomly varying AP but populating homogeneously all grid blocks with K_X and K_Y values. This is here called homogeneous permeability distribution. This unique value was randomly generated in accordance with the same lognormal distribution expressed in Table 1. This experiment will be called Case 2.a.

In parallel, another MC-DS procedure was executed incorporating different permeability values for each grid block (here called heterogeneous permeability distribution) which were generated using the SGS algorithm and honoring the same statistical model used for AP of its homogeneous counterpart. This experiment will be called Case 2.b.

Figure 4 shows the relative frequency histogram of gas production when permeability values were homogeneously distributed. Here, it can be noticed the range of production response is less than corresponding range for Case 1. However, this is not a completely fair comparison since other input parameters remained constant and could be influencing gas production response. The reported maximum value was 912,519.20 Mscf (less than maximum value obtained in Case 1), and central values are around of 304,000 Mscf (again, less than those central values of Case 1). From the CPD curve (here omitted), it was derived that probability of gas production being greater than 500,000 Mscf was 0.13. This value is substantially less than corresponding probability in Case 1, and can be an important difference when economical decisions are taken based on MS-DS indicators.

In Figure 5, other relative frequency histogram of gas production is shown. Now this plot corresponds to a heterogeneous distribution of permeability values on simulation grid produced by geostatistic algorithms (and respecting same previous constant values for the remaining input parameters). The maximum value for this case was 1,011,015.30 Mscf with central values around of 409,000 Mscf. Likewise, it could be derived that probability of gas production being greater than 500,000 Mscf is 0.26 (comparable with Case 1). All these statistical numbers overcome the previous results (Case 2.a) focused on only the homogeneous spatial distribution of random permeability values, and can lead to radically different decisions on a project.

Figure 6 shows superimposed cross-plots of AP values against corresponding cumulative gas production values for both cases 2.a and 2.b. Evidently, the higher AP is, the cumulative gas production is higher, which is not any surprise; nevertheless, a couple of notorious issues can be extracted from this graphic. The most important is that all gas production values obtained from dynamic simulations using permeability heterogeneously distributed (“blue” cloud), are greater than gas production values derived when permeability was homogeneously distributed into the DS grid (“pink” line). Both cross-plots tend to converge as the permeability increase.

Based on the reference mean value of 5 md, a vertical line was drawn on this graphic. This vertical line intersects the “pink” curve (no geostatistic) in a unique gas production value of 327,000 Mscf (rounded), but when it passes through the “blue” cloud (geostatistic) generates a range of higher gas production values between 420,000 Mscf and 470,000 Mscf. This observation is indicated here because all those gas production values that are related with these particular heterogeneous distributions of permeabilities

K_X and K_Y, have an average value (derived from all grid blocks) quite near to 5 md for the parameter AP. So we might affirm they are equivalent situations (from the AP value viewpoint) to the Case 2.a where permeabilities K_X and K_Y were homogeneously distributed with an AP value of 5 md.

In order to illustrate more this initial conclusion, we selected (for both cases) gas production values corresponding to AP values between 4.8 md and 5.2 md. A frequency histogram of gas production was generated superimposing results for both cases in Figure 7. Only 16 values of gas production were found under this condition when permeability was homogeneously distributed. All of them, concentrated between 310,000 Mscf and 330,000 Mscf. In contrast, 43 gas production responses were found under this condition for the heterogeneous situation, and they range between 390,000 Mscf and 510,000 Mscf. These numbers are obviously higher than those from the homogeneous case.

Finally, Figure 8 shows gas production history for three COMET3 simulations of gas production corresponding to three different geostatistical characterizations of permeability (G1, G2 and G3) which are different because were produced with different geostatistical parameters (nugget effect, range, etc.); however, all of them have the AP value of 5 md. In addition, it was plotted the production curve for the case of permeability homogeneously distributed with a constant AP value of 5 md (WOG). This figure is eloquent, and speaks by itself.

It has been seen that the range of variability of gas production appears richer and extended which means that better production scenarios were produced when the heterogeneous nature of permeability distribution in reservoirs was included. This is an important difference in comparison with results based on the homogeneous spatial distribution of permeability.

The use of a lognormal distribution as the permeability statistical behavior, and the fact that geostatistical algorithms can generate higher permeability values to feed some grid blocks constitute factors which favors gas production[9, 10]. In addition, these high permeability values could be connected each other in space generating preferential flow paths which also can favor gas production.

This new spectrum of possible production responses has direct implications on feasibility studies about exploitation of unconventional plays. Important indicators like average production, extreme values or probabilities (for instance, production being greater than a specified threshold) are often utilized for making decisions and are very sensitive to the greater variability obtained with the use of geostatistical characterizations. So it is important to keep exploring the effects on risk and economical analyses that geostatistical characterizations have.

Figure 9 presents a Tornado plot for sensitivity analysis. Two important aspects are revealed in this graphic. Firstly, the most impacting parameter upon gas production is the AP. And secondly, its impact is of such a nature that completely overshadows the influence of geostatistical factors.

A possible explanation is linked with the basic conditions conceived for these experiments, i.e., reservoir conditions completely symmetric (square region with only a producer well in the middle) and a treatment like a two-dimensional study. So from these first experiences it might be concluded that essential parameters in the geostatistical characterization of a reservoir can be ignored. However, we believe this would be a premature conclusion.

These comparative results (and the next ones) have been summarized in Table 2.

Case Study 3

(Homogeneous and heterogeneous permeability distribution, and inclusion of variable porosity)

This case is similar to the previous one except for the incorporation of porosity as a stochastic variable. Note that AP and FP were considered statistically independent.

Base values (either the most likely or mean value) were adopted for all uncertain parameters except AP and FP which were varied randomly in accordance with the same distributions expressed in Table 1. Firstly, spatial distribution of these variables into the grid was carried out without using geostatistical simulation, i.e., in a homogeneous manner. This first experiment will be here called Case 3.a.

In general terms, the inclusion did not cause relevant impacts on the stochastic behavior of gas production. The relative frequency histogram of gas production when these particular reservoir parameters are homogeneously distributed is shown in Figure 13. When compared with results derived in Case 1 (Fig. 1) and Case 2.a for the equivalent situation (Fig. 4), it can be noticed similar statistical behavior of the corresponding production responses. The present range of variability and maximum simulated value (972,841.20 Mscf) are in the same order of magnitude. However, central values of gas production in this case were around of 310,000 Mscf, which is notoriously less than the value obtained in Case 1 (370,000 Mscf) where all variables were randomly changed and homogeneously distributed. Indeed, mean and median values reflect this situation (Table 2). This means that more simulations of lower gas production were produced as a consequence of alternative combinations of AP and FP. When central values of this Case 3.a are compared with those derived in the equivalent situation of Case 2.a (around to 304,000 Mscf), more similarity can be found.

Analyzing the CPD curve for this case (here omitted), the value obtained for probability of gas production being greater than 500,000 Mscf was 0.17, which is relatively similar to the value 0.13 obtained in the equivalent situation of Case 2.a. When comparing with those values obtained in Case 1 and Case 2.b (permeability heterogeneously distributed), this value results substantially less.

For the geostatistical version of this case (called Case 3.b) we have frequency histogram of gas production shown in Figure 14. This plot corresponds only to gas production values associated with heterogeneous distributions of permeability. FP was randomly varied but homogeneously distributed in grid blocks, and same previous constant values were used for the remaining input parameters.

The range of variability of gas production is again greater than the homogeneous case although no significantly. However, higher production scenarios were produced when the heterogeneous nature of permeability distribution in reservoirs was included. Indeed, the maximum value for this case was 1,243,013.00 Mscf with central values around of 420,000 Mscf. Comparing now both situations of this Case Study 3, the maximum value of Case 3.b is certainly greater than value 972,841.20 Mscf obtained when permeability is distributed homogeneously but it can explained by same arguments given in the Case Study 2 about the geostatistical appearance of high permeability values and/or their possible connectivity.

It is necessary to remind that production gas is being interpreted as a random variable and all simulated values, including maximum one, must be conceived only as possible events with their respective probabilities of occurrence.

From the analysis of the CPD curve (here omitted), it was inferred that probability of gas production being greater than 500,000 Mscf was 0.30. All these statistic numbers are the highest values of these experiments linked to the permeability variability (see Table 2). The MC-DS procedure run for these conditions was able to generate combinations of AP and FP values which led to more variable production possibilities.

Finally, Figure 12 shows the Tornado plot derived for this geostatistic experience. This graphic reinforces the aspects already concluded about geostatistical parameters when they are compared with the influence of analyzed reservoir parameters (Case 2.b). Again, the most impacting parameter upon gas production was the AP followed by FP. Their superlative influence on gas production darkens the influence of geostatistical factors.

Case Study 4

(Heterogeneous permeability distribution)

In order to have the counterpart of Case 1, a MC-DS procedure was applied where all selected reservoir parameters were randomly varied but now including permeability heterogeneously distributed. Again, all input parameters were randomly varied according their respective statistical models (Table 1) and, in particular, permeability was heterogeneously distributed on grid blocks.

When a Tornado plot about sensitivity of cumulative gas production is generated (Figure 13), AP and FP are again identified as main performance drivers, and the influence of geostatistical parameters is once again a minor issue.

Figure 14 shows the relative frequency histogram of cumulative total gas with its summary statistical values. In this case, we obtained a maximum simulated value of 1,123,267.50 Mscf which is in the same order of magnitude of Case 2.b when AP was the only changing variable and was also being heterogeneously distributed into the reservoir grid. Besides, this maximum value is in the same order of magnitude as both situations of Case 3 when FP was incorporated. These results are consistent with the fact, concluded from Case 1 and Case 3, that AP and FP are forcefully impacting gas production events. They not only darkness the influence of geostatistical parameters but also minimizes the effect caused by other volatile parameters.

Central values (mean and median) of gas production values are around 362,000 Mscf and are similar to those obtained in Case 1. From the corresponding CPD curve (here omitted), it was inferred that probability of gas production being greater than 500,000 Mscf was 0.19. This value is less than 0.24 from its counterpart Case 1 and also less than 0.26 (Case 2.b) and 0.30 (Case 3.b) where geostatistical distributions were also applied with different conditions.

Reviewing all frequency histograms till now analyzed, we can see that all of them present distributions positively skewed, which is mainly due to the influence that AP (lognormally distributed) has had on production responses. For this type of positively skewed distributions, the median value is usually accepted as a more representative central value (average) of the statistical behavior of the variable. In consequence, when we look at Table 2, it is particularly notorious the substantial difference between median values of Case 2.a (292,214 Mscf) and Case 3.a (291,450 Mscf), both without geostatistics, and their counterpart median values (using geostatistics) of Case 2.b (408,781 Mscf) and Case 3.b (407,090 Mscf). Again, it seems that inclusion of heterogeneously distributed permeability has favored the gas production. Median value of Case 1 (355,526 Mscf) and its counterpart median for Case 4 (353,198 Mscf) are practically identical.

Case Study 5

(Homogeneous and heterogeneous porosity distribution)

This final case is focused on the random variability of parameter FP, on how FP values are spatially utilized in the simulation grid, and how the production response is affected. Again, base values were adopted for all uncertain parameters but FP.

Initially, a conventional MC-DS procedure was executed where FP was randomly varied and their values were homogeneously distributed in all grid blocks. In other words, Case 5.a is defined by a homogeneous distribution of FP into the simulation grid. The value randomly generated is in accordance with the same normal distribution expressed in Table 1.

In parallel, another MC-DS procedure was executed incorporating different FP values for each grid block (heterogeneous porosity distribution), which were generated using the SGS algorithm and honoring the same statistical model used for FP in its homogeneous counterpart (Case 5.a). This experiment will be here called Case 5.b.

Results for this case study were somewhat singular. Figure 15 and Figure 16 show relative frequency histograms of gas production for Case 5.a and Case 5.b respectively. Both histograms present a more reduced range of production responses when are compared with all previous cases. Reported maximum values were 880,168.60 Mscf and 853,658.10 Mscf respectively, which constitutes the least values of all reported maximum ones. Besides, reported standard deviation values (106,159 Mscf and 97,238 Mscf respectively) also constituted the least values of all reported standard deviations, which reinforce the previous observation of having a least spectrum of variability for gas production response in this experiment. However, these facts could be explained if we remind the stochastic origin of FP values: a normal distribution.

Comparing Case 5.a with Case 2.a and Case 5.b with Case 2.b (same experiment conditions but AP and FP exchanging roles), we can notice that median and mean values of both situations of Case Study 5 are greater than corresponding ones of both cases in Study 2 (Table 2). Moreover, median and mean values of Case 5.b were the greatest values of all reported central ones.

Another remarkable result was the minimum value obtained in Case 5.b, i.e., 357,442 Mscf. When it is compared with different indicators of previous cases (minimum and central values), it might be said that is an optimistic result (instead of being a minimum one). Due to this “high” minimum value and the more reduced spectrum of gas production variability, we found another high indicator for Case 5.b: the probability of gas production being greater than 500,000 Mscf is 0.69. This particular probability can substantially change the success of an exploitation project if decisions are based on it. The corresponding probability of gas production being greater than 500,000 Mscf for Case 5.a is 0.10, which is the lowest probability of these experiments but in the same order of magnitude of Case 2.a.

In order to compare gas production behavior for both case studies (5.a and 5.b), superimposed cross-plots of FP values against corresponding cumulative gas production values were plotted in Figure 17. Again no surprises: the higher FP is the cumulative gas production is lower (and vice versa). The most relevant issue derived from this graphic is all gas production values coming from simulations with porosity heterogeneously distributed (“blue” cloud), are considerably greater than gas production values derived when porosity was homogeneously distributed (“pink” line). Both cross-plots tend to converge when the porosity goes to 0.0 although both production behaviors were well distanced.

Based on the porosity reference value of 0.005, a vertical line was drawn on this graphic. This vertical line intersects the “pink” curve (without geostatistics) in a unique gas production value of 327,000 Mscf (which coincides with Case 2.a), but when it passes through the “blue” cloud (with geostatistics), generates a range of higher gas production values between 500,000 Mscf and 600,000 Mscf. All these gas production values inside this range (associated to these particular heterogeneous distributions of FP) have an average FP value (derived from all grid blocks) quite near to 0.005. So again we might accept them as equivalent situations (from the FP value point of view) to the Case 5.a where FP was homogeneously distributed with a FP value of 0.005.

A possible explanation for this value superiority, it can be extracted from Figure 17. From both behaviors (“pink” line and “blue” cloud), we can conclude that change rates of gas production are more marked as FP values are being diminished than as they are being incremented. This fact implies that for lower values of FP, we have a greater impact in the increment of gas production than the influence caused by

the presence of greater values of FP in the decrease of gas production. So when heterogeneous values of FP are geostatistically distributed into the grid, it is reasonable to hope that gas production should be greater due to the presence of FP low values in the grid.

Again, higher production scenarios have been produced when the heterogeneous nature of FP distribution was included. This result constitutes a relevant difference when we compare with those results based on the homogeneous manner of spatially distributing the parameter FP. As it was concluded before, this new spectrum of possible production responses has direct consequences on decisions about exploitation of unconventional plays.

In Figure 18, the corresponding Tornado plot for Case 5.b is shown. Again, the most impacting parameter upon gas production is the parameter FP being of such a nature that completely devaluates the influence of geostatistical parameters. We still believe that basic conditions conceived for these experiments are the cause of these results.

So it is necessary to continue exploring the effects that geostatistical characterizations in these MC-DS procedures and consequently on risk and economical analyses. In particular, a future research has been programmed where FP will be randomly varied and heterogeneously distributed in grid blocks simultaneously with AP and with different grades of interdependence.

CONCLUSIONS

- Geostatistical distributions of K_X and K_Y permeabilities (only) lead to higher gas production than homogeneous permeability distribution.

- Geostatistical distributions of Fracture Porosity values (only) also lead to the occurrence of higher gas production responses.

- In examples here developed, no geostatistical parameter stood out in its influence on production response.

- In examples here developed, a conventional MC-DS procedure applied to all the parameters turned out to be equivalent, in its results, to the obtained ones when geostatistical distributions of permeability were included.

- The use of geostatistical characterizations of Average Permeability and Fracture Porosity in a MC-DS procedure impacts the production response. Consequently, impacts making-decisions process in exploitation projects.

REFERENCES

1. Nakayama, K.: “Estimation of Reservoir Properties by Monte Carlo Simulation,” Paper SPE 59408 presented at the 2000 SPE Asia Pacific Conference on Integrated Modeling for Asset Management held in Yokohama, Japan, April 25-26, 2000.
2. Sawyer, W.K., Zuber, M.D. and Williamson, J.R.: “A Simulation-Based Spreadsheet Program for History Matching and Forecasting Shale Gas Production,” Paper SPE 57439 presented at the 1999 SPE Eastern Regional Conference and Exhibition held in Charleston, West Virginia, Oct. 21-22, 1999.
3. MacMillan, D.J., Pletcher, J.L. and Bourgeois, S.A.: “Practical Tools to Assist History Matching,” Paper SPE 51888 presented at the 1999 SPE Reservoir Simulation Symposium held in Houston, TX, Feb. 14-17, 1999.
4. Roadifer, R. D., Farnan, R. A., Krabtree, B. J., Raterman, K. T., Moore, T. R., “History Matching (Reservoir Parameter Estimation) for Coalbed Methane Reservoirs via Monte Carlo Simulation,” presented at the 2003 International Coalbed Methane Symposium , Tuscaloosa, Alabama, May 5-9.
5. Oudinot, A.Y., Koperna, G.J. and Reeves, S.R., “Development of a Probabilistic Forecasting and History Matching Model for Coalbed Methane Reservoirs”, presented at the 2005 International Coalbed Methane Symposium, Tuscaloosa, Alabama, May 5-9.
6. Portella, R.C.M. and Prais, F. (Petrobras), “Use of Automatic History Matching and Geostatistical Simulation to Improve Production Forecast,” SPE 53976 presented at the 1999 SPE Latin America and Caribbean Petroleum Engineering Conference, Caracas, Venezuela, 21-23 April.
7. Bennett, F, and Graf, T. (Schlumberger), “Use of Geostatistical Modeling and Automatic History Matching to Estimate Production Forecast Uncertainty,” SPE 74389 presented at the 2002 SPE International Petroleum Conference and Exhibition, Villahermosa, Mexico, 10-12 February.
8. White, C.D., Willis, B.J, Narayanan, K., and Dutton, S.P. “Identifying Controls on Reservoir Behavior Using Designed Simulations”. SPE 62971, presented at the 2000 SPE Annual Technical Conference and Exhibition, Dallas, Texas, Oct. 1-4. 9.
9. Deutsch, C.V. and Journel, A.G., “GSLIB: Geostatistical Software Library and User’s Guide. Oxford University Press, 1998
10. Goovaerts, P., “Geostatistics for Natural Resources Evaluation”. Oxford University Press, 1997

Table 1: Statistical models for each parameter

Parameter	Units	Distribution
Initial Water Saturation	fraction	T(0.7, 1,1)
Average Permeability	md	L(5,2)
Permeability Anisotropy Factor	dimensionless	T(1,2,5)
Fracture Porosity	fraction	N(0.005, 0.002)
Sorption Time	days	T(30, 300, 3000)
Fracture Spacing	inches	T(12, 36, 120)
Langmuir Volume	cuft/cuft	T(3.82, 6.82, 9.82)
Langmuir Pressure	psi	T(300, 354, 400)
Water Density	lb/ft	T(43.2, 50.42, 57.63)
Skin Factor	dimensionless	T(-4, 0, -2)
Desorption Pressure Function	dimensionless	T(0.7, 1,1)
Irreducible Water Saturation	fraction	T(0.1, 0.2, 0.3)
Maximum gas relative permeability	dimensionless	T(0.5, 0.75, 1)
Corey gas exponent	dimensionless	T(1, 2, 3)
Corey water exponent	dimensionless	T(1, 2, 3)

Table 2: Quantitative summary of statistical indicators

Case	Geostat.	Average Perm.	Fracture Porosity	Other Variables	Minimum (Mscf)	Median (Mscf)	Mean (Mscf)	Maximum (Mscf)	Standard Deviation	Probability (500,000)
1	Off	Variable	Variable	Variable	51,0945	355,526	385,804	1,142,974	196,819	0.24
2.a	Off	Variable	Constant	Constant	70,214	292,214	316,299	912,520	149,613	0.13
2.b	On	Variable	Constant	Constant	129,208	408,781	410,392	1,011,015	139,234	0.26
3.a	Off	Variable	Variable	Constant	35,614	291,450	330,753	972,841	185,655	0.17
3.b	On	Variable	Variable	Constant	68,928	407,090	435,107	1,243,013	180,201	0.30
4	On	Variable	Variable	Variable	14,148	353,198	371,697	1,123,267	174,112	0.19
5.a	Off	Constant	Variable	Constant	156,691	328,183	350,254	880,169	106,159	0.10
5.b	On	Constant	Variable	Constant	357,442	546,156	559,390	853,658	97,238	0.69

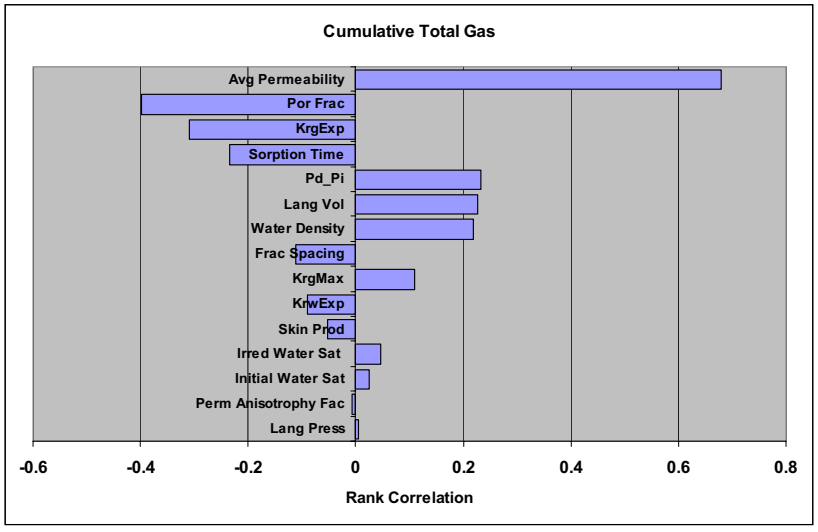

Figure 1: Tornado Plot of Cumulative Total Gas (Case 1, without geostatistics)

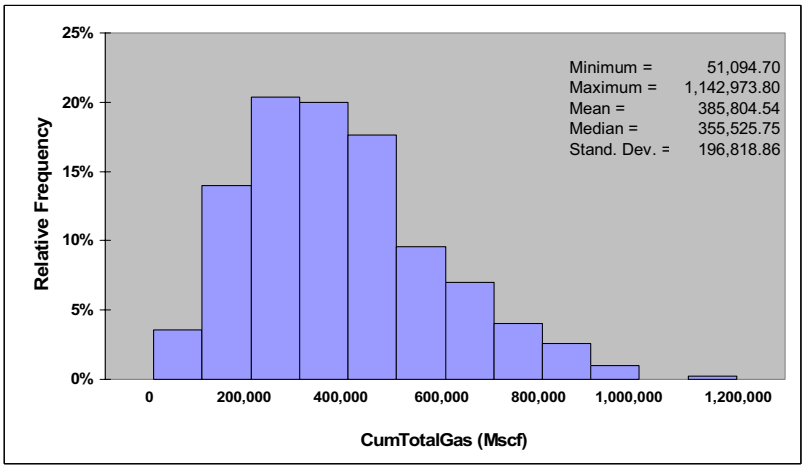

Figure 2: Frequency Histogram of Gas Production (Case 1)

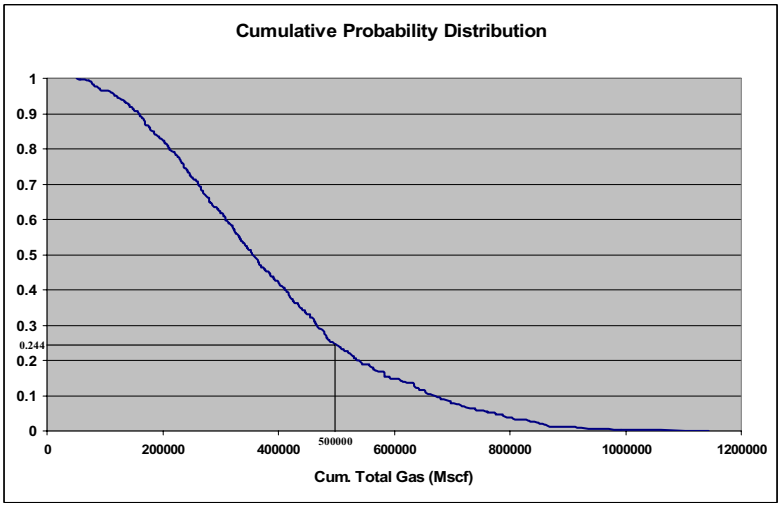

Figure 3: Cumulative Probability Distribution of Gas Production (Case 1)

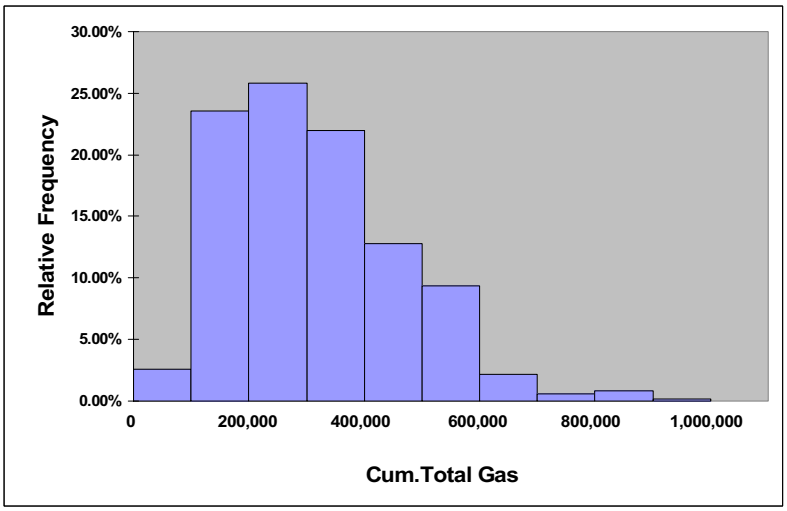

Figure 4: Frequency Histogram of Gas Production (Case 2.a, without geostatistic)

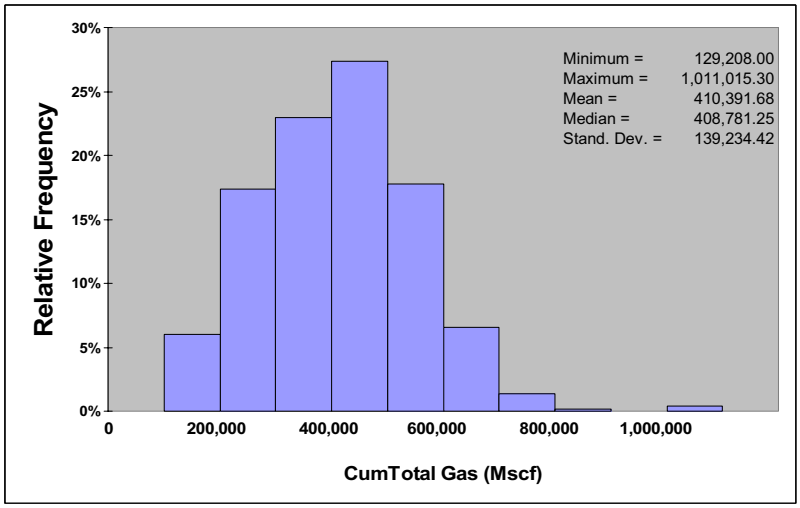

Figure 5: Frequency Histogram of Gas Production (Case 2.b, with geostatistic)

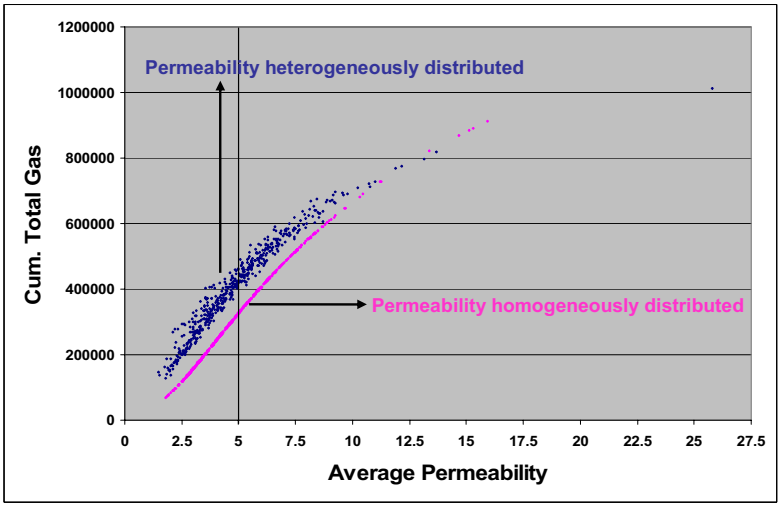

Figure 6: Cross-plot of Cumulative Total Gas vs. Average Permeability (Case 2.a & Case 2.b)

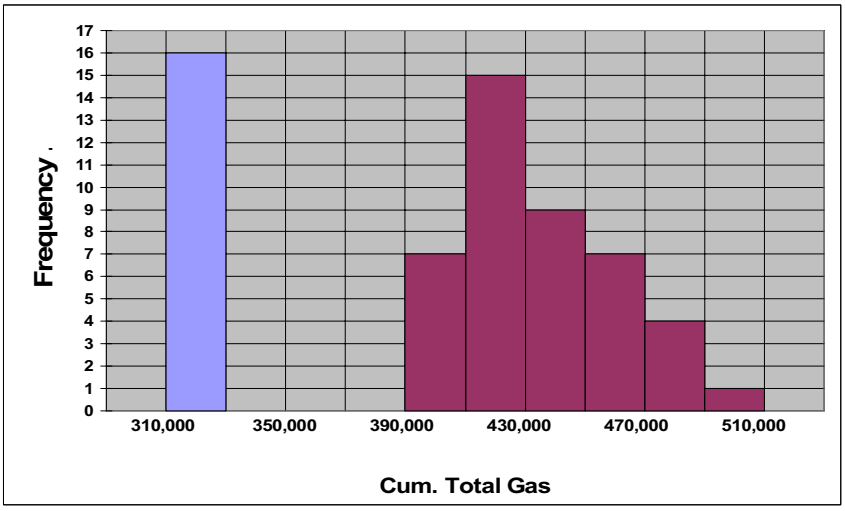

Figure 7: Conditioned frequency histogram of Cumulative Total Gas (Case 2.a & Case 2.b)

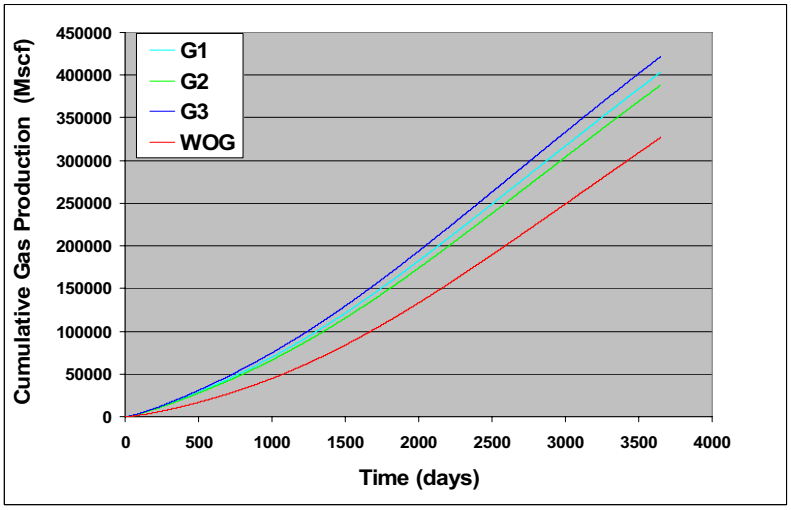

Figure 8: Selected gas production histories: Case 2.a (WOG) and Case 2.b (G1, G2 & G3)

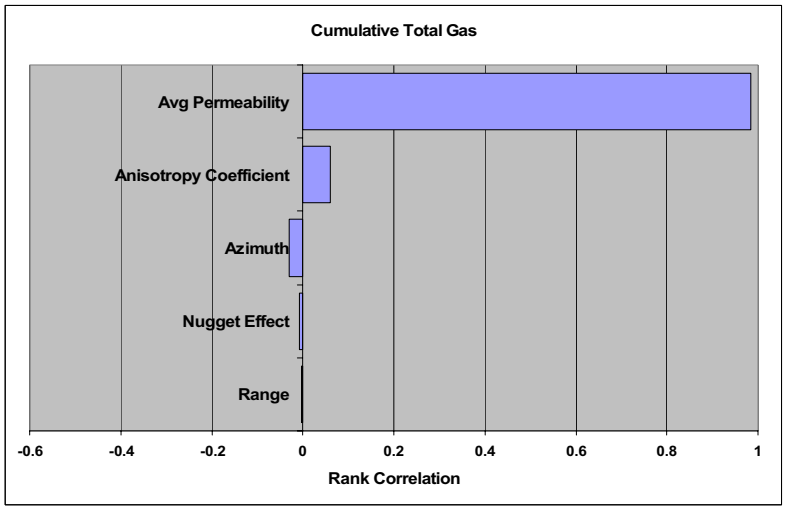

Figure 9: Tornado Plot of Cumulative Total Gas (Case 2.b, with geostatistic)

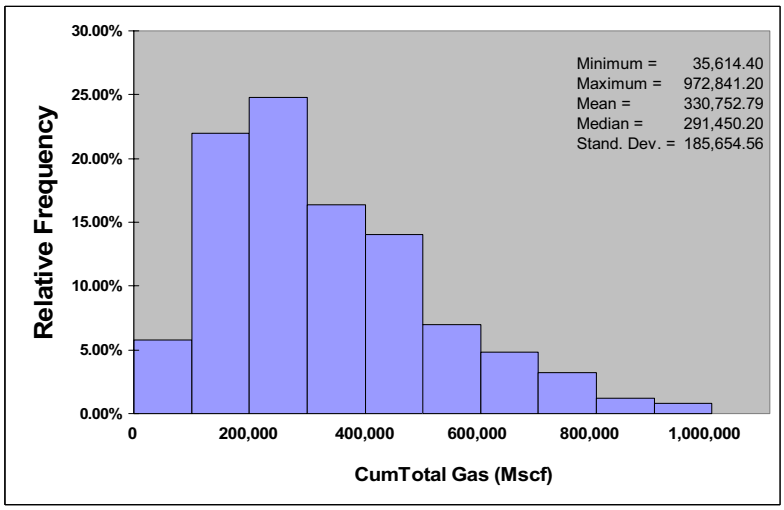

Figure 10: Frequency Histogram of Gas Production (Case 3.a, without geostatistic)

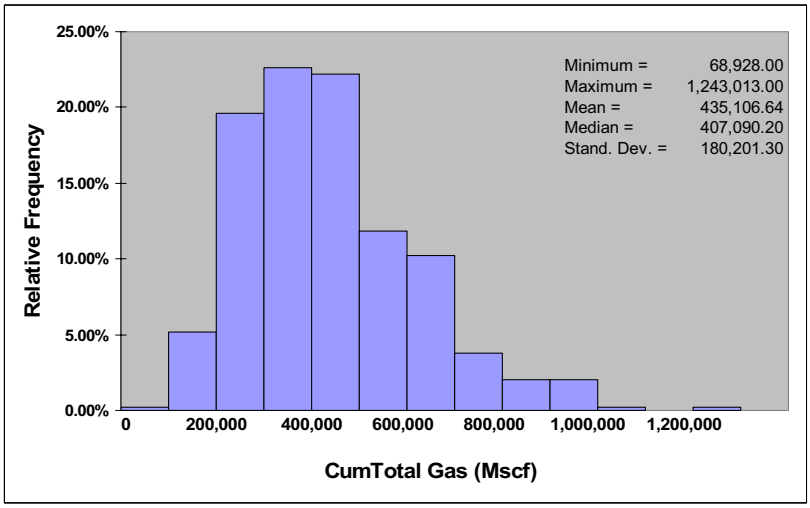

Figure 11: Frequency Histogram of Gas Production (Case 3.b, with geostatistic)

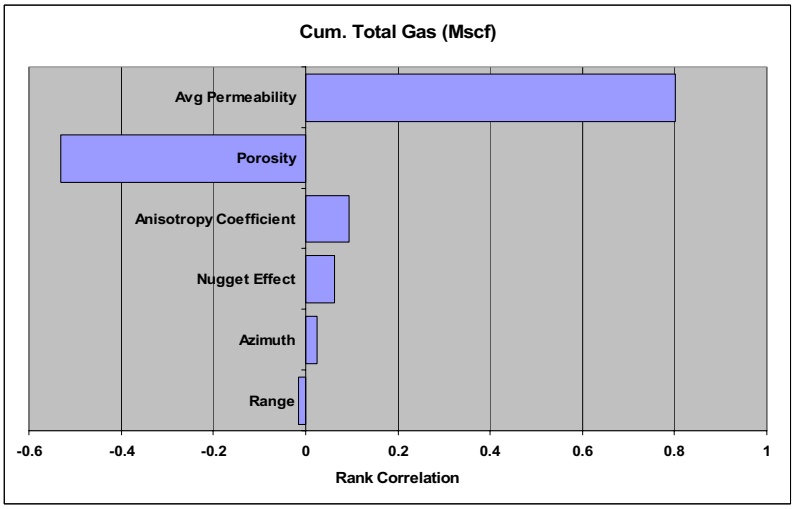

Figure 12: Tornado Plot of Cumulative Total Gas (Case 3.b, with geostatistic)

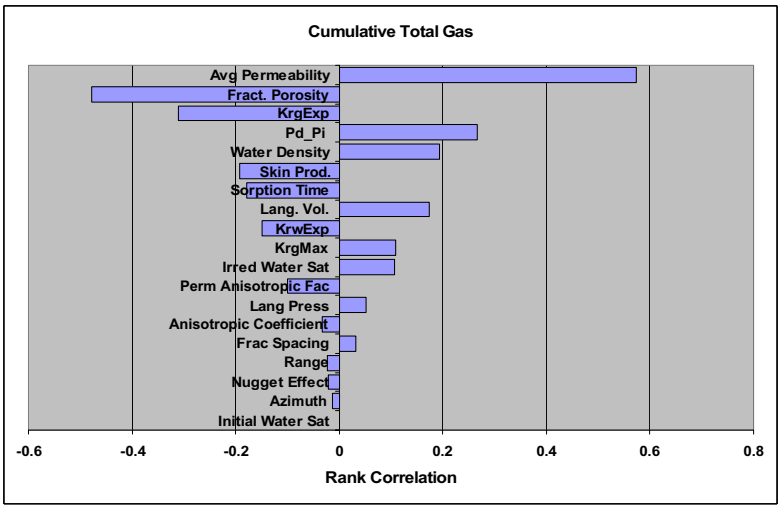

Figure 13: Tornado Plot of Cumulative Total Gas (Case 4, with geostatistic)

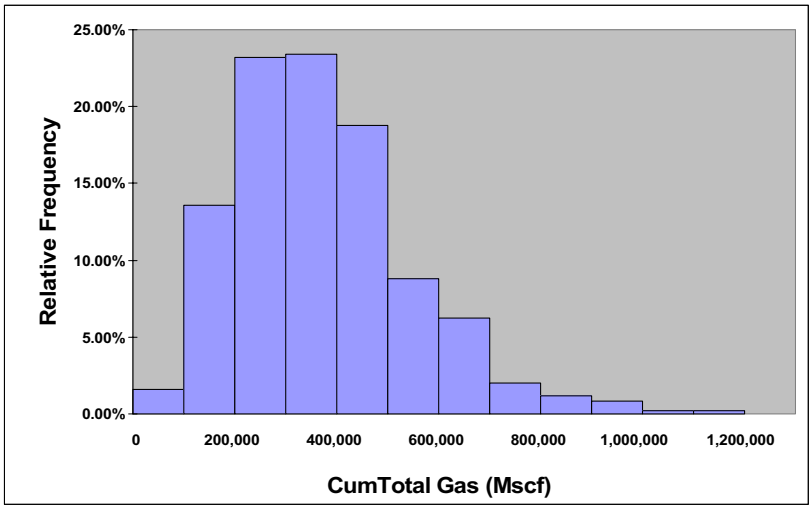

Figure 14: Frequency Histogram of Gas Production (Case 4, with geostatistic)

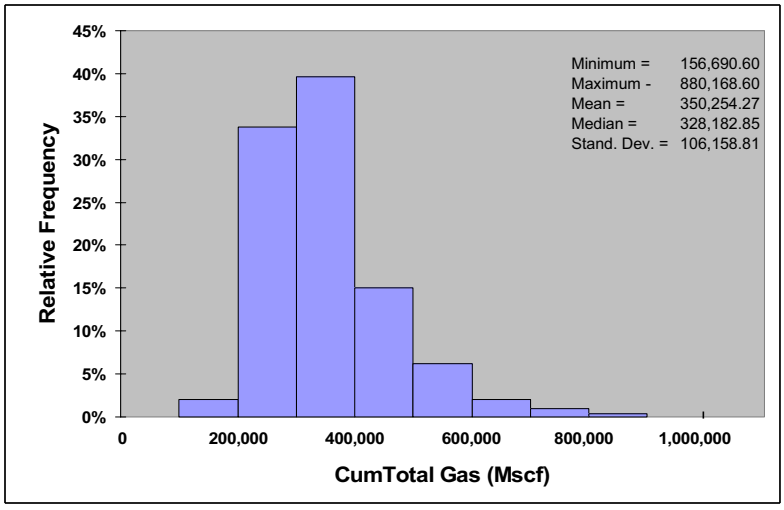

Figure 15: Frequency Histogram of Gas Production (Case 5.a, without geostatistic)

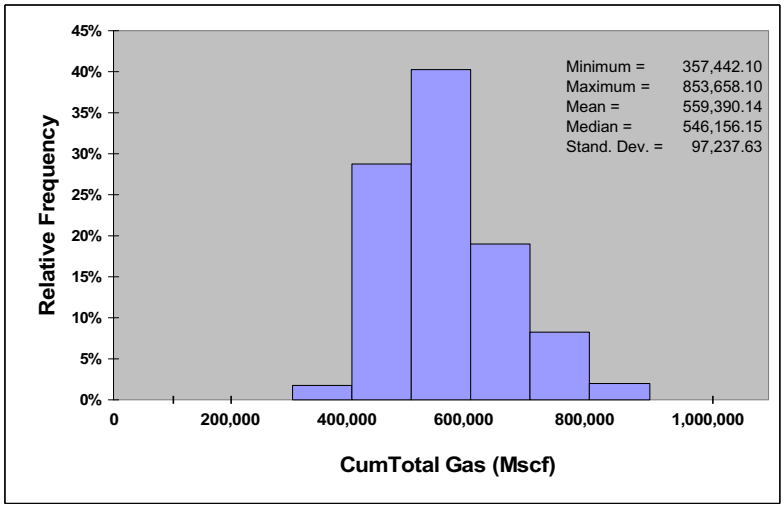

Figure 16: Frequency Histogram of Gas Production (Case 5.b, without geostatistic)

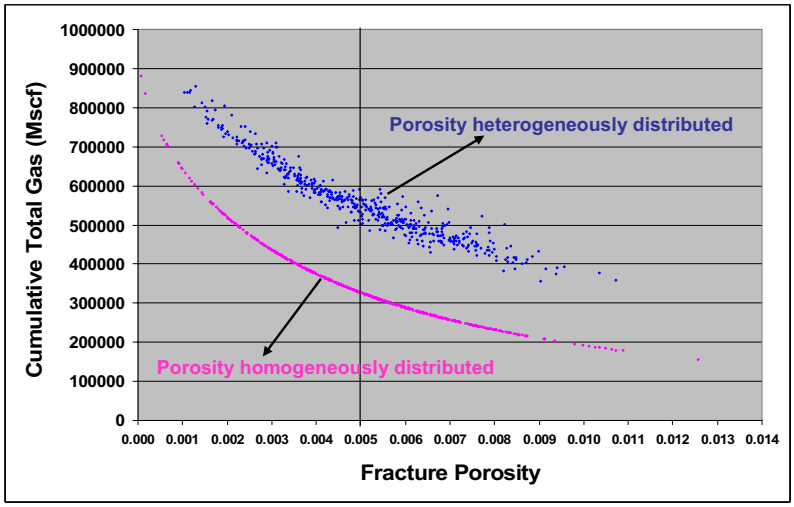

Figure 17: Cross-plot of Cumulative Total Gas vs. Fracture Porosity (Case 5.a & Case 5.b)

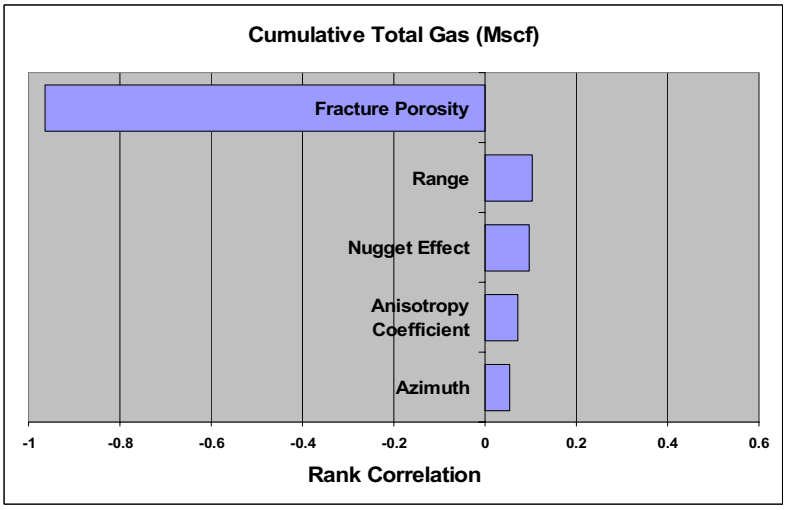

Figure 18: Tornado Plot of Cumulative Total Gas (Case 5.b, with geostatistic)